Aging-related genes related to the prognosis and the immune microenvironment of acute myeloid leukemia

dongxu Gang
The First Affiliated Hospital of Wenzhou Medical University
yinyan Jiang
Wenzhou Medical University First Affiliated Hospital: The First Affiliated Hospital of Wenzhou Medical University
xiaofang Wang
Wenzhou Medical University First Affiliated Hospital: The First Affiliated Hospital of Wenzhou Medical University
jifan Zhou
Wenzhou Medical University First Affiliated Hospital: The First Affiliated Hospital of Wenzhou Medical University
xiaoyuan Zhang
Wenzhou Medical University First Affiliated Hospital: The First Affiliated Hospital of Wenzhou Medical University
xiaoyu He
Wenzhou Medical University First Affiliated Hospital: The First Affiliated Hospital of Wenzhou Medical University
rujiao Dong
Wenzhou Medical University First Affiliated Hospital: The First Affiliated Hospital of Wenzhou Medical University
ziyang Huang
Wenzhou Medical University First Affiliated Hospital: The First Affiliated Hospital of Wenzhou Medical University
songfu Jiang (✉ 1837904019@qq.com)
Wenzhou Medical University First Affiliated Hospital: The First Affiliated Hospital of Wenzhou Medical University https://orcid.org/0000-0002-1458-1753

Research Article

Keywords: Acute myeloid leukemia, Aging, Biomarker, UCP2, Genipin, Prognosis

Posted Date: November 14th, 2022

DOI: https://doi.org/10.21203/rs.3.rs-2245364/v1

Aging-related genes related to the prognosis and the immune microenvironment of acute myeloid leukemia

Dongxu Gang[1#], Yinyan Jiang [1#], Xiaofang Wang[1], Jifan Zhou[1], Xiaoyuan Zhang[1], Xiaoyu He[1], Rujiao Dong[1], Ziyang Huang[1*], Songfu Jiang[1*]

[1]Department of Hematology, The First Affiliated Hospital of Wenzhou Medical University, Wenzhou, Zhejiang, China

*** Correspondence:**

Ziyang Huang

hzy9@wzhospital.cn

Songfu Jiang

1837904019@qq.com

[#]These authors have contributed equally to this work

Abstract

Background: Acute myeloid leukemia (AML), one of the most common malignancies of the hematologic system, has progressively increased in incidence. Aging is present in both normal tissues and the tumor microenvironment. However, the relationship between senescence and AML prognosis is still not elucidated.

Methods: In this study, RNA sequencing data of AML were obtained from TCGA, and prognostic prediction models were established by LASSO-Cox analysis.

Differences in immune infiltration between the different risk groups were calculated using the CIBERSORT and ESTIMATE scoring methods. The KEGG and GO gene enrichment and GSEA enrichment were also used to enrich for differential pathways between the two groups. Subsequently, this study collected bone marrow samples from patients and healthy individuals to verify the differential expression of uncoupling protein 2 (UCP2) in different populations. Genipin, a UCP2 protein inhibitor, was also used to examine its effects on proliferation, cell cycle, and apoptosis in AML cell lines in vitro.

Results: It showed that Aging-related genes (ARGs) expression was correlated with prognosis. And there was a significant difference in the abundance of immune microenvironment cells between the two groups of patients at high risk and low risk. Subsequently, UCP2 expression was found to be elevated in AML patients. Genipin inhibits UCP2 protein and suppresses the proliferation of AML cell lines in vitro.

Conclusion: ARGs can be used as a predictor of prognosis in AML patients. Moreover, suppressing UCP2 can reduce the proliferation of AML cell lines, alter their cell cycle and promote apoptosis in vitro.

Keywords: Acute myeloid leukemia[1], Aging[2], Biomarker[3], UCP2[4], Genipin[5], Prognosis[6].

1 Introduction

AML, one of the most common hematologic malignancies, is usually characterized by

the accumulation of myeloid progenitor cells in the bone marrow and peripheral blood and has a very poor prognosis. Although many different treatments are available, studies have shown that the five-year survival rate for AML is only 24%. The main treatment remains chemotherapy, but resistance mechanisms are very common in AML, and the transition to drug resistance in patients after chemotherapy is a major focus and difficulty in the treatment of AML, and there is now a lot of literature on the different resistance mechanisms(1). However, the prognostic guidelines for AML are not uniform, and this calls for research to explore more prognostic signatures. With the development of bioinformatics, we can use new methods to provide more clinical guidance for survival prediction and therapeutic target selection(2, 3).

Prolongation or blockage of the cell cycle caused by various factors such as hypoxia, injury, and cancer is defined as cellular senescence(4). Indeed, cells undergo senescence regardless of their age. Although cellular senescence in tumors can also play a role in tumor suppression and tissue repair, studies have also demonstrated that this process can promote tumor proliferation, invasion, etc(5, 6). Senescent cells can secrete more cytokines, chemokines, growth regulators, and other factors(7). This feature mediates many of the physiological and pathological effects of senescent cells.

ARGs remain unstudied in AML, although they have been used to predict disease prognosis(8). The prognostic role of ARGs and their mechanism of action remain unclear.

UCP2 is a mitochondrial protein that controls the production of reactive oxygen species (ROS) and regulates mitochondrial function(9). It is commonly studied in non-tumor

diseases such as diabetes and obesity. Recently, it has been shown to have antitumor effects in a variety of cancers(10-12). However, there is still a gap in the field of research on AML.

This study investigated the prognostic value of ARGs in AML. Transcriptomic datasets of AML were downloaded from The Cancer Genome Atlas (TCGA) as well as Gene Expression Omnibus (GEO) databases. The prognostic impact of ARGs on AML was first assessed using a one-way Cox regression analysis. The least absolute shrinkage and selection operator (LASSO) Cox regression was performed to construct risk profiles associated with ARGs in AML patients. The accuracy of the risk profile was also verified, and the results showed that it was a valid predictor of patient prognosis. According to the risk grouping, the abundance of tumor-infiltrating immune cells differed significantly among different groups. The results of the validation analysis were analyzed and drugs targeting one of the UCP2 proteins were identified.

2 Article types

ORIGINAL RESEARCH

3.1 Materials and Methods

3.1.1 Acquisition of ARGs

ARGs were collected from the GeneCards database (https://www.genecards.org/), which provides comprehensive information on human genes. The term "aging" was used as a keyword search, and genes with a correlation score >8 were filtered as ARGs

in the results.

3.1.2 Collection of data sets

We collected 200 available samples from The Cancer Genome Atlas (TCGA), including level three RNA-seq expression data from 132 patients. All samples enrolled in the cohort ensured appropriate prognostic data and other clinical information. These data were used as a training cohort. The microarray data and corresponding survival information for the remaining 510 samples were obtained from 2 different Gene Expression Omnibus (GEO) datasets. 510 samples from GSE12417 and GSE71014 were included and again ensured that the corresponding clinical information and prognostic data were included for all samples before use.

3.1.3 DEG Analysis

First, 9325 genes were found to be associated with prognosis in AML by univariate COX regression. And then the intersection of differential genes with the collected aging genes was taken to obtain 75 aging genes associated with AML prognosis.

3.1.4 Building and validating the risk model

Then we used the LASSO regression method to construct the obtained prognosis-related ARGs as a multivariate model of ARGs. Risk scores were calculated for each patient in the training and validation cohorts. Median values were used to classify patients into high or low-risk groups. Meanwhile, Kaplan–Meier survival analysis was constructed and the log-rank test was used to assess overall survival (OS) between

groups. The sensitivity and specificity of prognostic performance were viewed by receiver operating characteristic (ROC) curves. The area under the curve (AUC) values indicated discrimination.

3.1.5 Tumor immune microenvironment landscape and its potential impact on immunotherapy

CIBERSORT was used to calculate the infiltration abundance of 22 immune cell types in AML patients, grouped according to high-and low-risk populations. ESTIMATE scores of immune cells, stromal scores, immune scores, and tumor purity in AML patients were estimated using the ESTIMATE algorithm. Six immune cell abundances were also calculated using the EPIC score. Samples with $P < 0.05$ were selected for further analysis.

3.1.6 Functional enrichment analysis

Gene enrichment analysis is an important tool to integrate genes with function, and gene set enrichment analysis (GSEA) annotation was used to find potential mechanisms of aging-related genes in AML. We used both gene ontology (GO) and the Kyoto encyclopedia of genes and genomes (KEGG) to identify which molecular mechanisms differ between high-risk and low-risk patients.

3.1.7 UCP2 pan-cancer analysis

We downloaded the uniformly normalized pan-cancer dataset: TCGA TARGET GTEx (PANCAN, N=19131, G=60499) from the UCSC (https://xenabrowser.net/) database,

from which we further extracted the expression data of ENSG00000175567 (*UCP2*) gene in each sample. And further, we screened the samples from the following sources: Solid Tissue Normal, Primary Solid Tumor, Primary Tumor, Normal Tissue, Primary Blood-Derived Cancer - Bone Marrow, and Primary In addition, we filtered samples with an expression level of 0 and further log2(x+0.001) transformed for each expression value, and finally, we eliminated those with less than 3 samples in a single cancer species to obtain expression data for 34 cancer species. We then analyzed the relationship between *UCP2* and the prognosis of various tumors and the correlation with immunomodulatory genes, respectively. Then, we calculated the relationship between gene expression and tumor stemness(13).

3.1.8 Reverse transcription-polymerase chain reaction (RT-PCR)

Total RNA extraction using Trizol reagent (Life Technologies) for reverse transcription-polymerase chain reaction (RT-PCR). Transcription amplification was performed using an RT-PCR kit (Life Technologies). PCR amplification was performed using the following primers: *UCP-2*, forward: 5′-CCCCGAAGCCTCTACAATGG-3′, reverse: 5′-CTGAGCTTGGAATCGGACCTT-3′, *GAPDH*, forward: 5′-GGAGCGAGATCCCTCCCCAAAAT-3′ and reverse: 5′-GGAGCGAGATCCCTCCAAAAT -3 '.

3.1.9 Clinical samples and qRT-PCR analysis

Bone marrow samples were obtained from 19 AML patients and 19 healthy donors from the First Hospital of Wenzhou Medical University. Our study was approved by

the ethics committee of the First Hospital of Wenzhou Medical University1. Quantitative real-time PCR (qRT-PCR) total RNA was extracted using TRIZOL reagent (Life Technologies). reverse transcription was then performed using the HiScript Q RT SuperMix kit (Vazyme, Nanjing, China). qRT-PCR was performed on an Applied Biosystems Quantstudio 6Flex qRT-PCR using a SYBR probe (Applied Biosystems, Foster City, CA, USA). then, qRT-PCR was performed to assess mRNA expression using SYBR Green Master Mix (CWBIO, Jiangsu, China) in an Applied Biosystems QuantStudio 3 Real-Time PCR System (Thermo Fisher Scientific, MA, USA) as previously described.

3.1.10 Cell culture

Cell culture of human leukemia cells HL-60, Kasumi-1 cell line was purchased from BNCC (Henan, China) and maintained according to the manufacturer's instructions. We have confirmed the cell lines used in the experiments by specialized STR analysis and tested them for mycoplasma contamination. Cells were grown in RPMI1640 medium (meilunbio, Dalian, China) containing 10% fetal bovine serum (FBS, meilunbio, Dalian, China).

3.1.11 Cell viability assay

Cell proliferation was determined by Cell Counting Kit-8 (meilunbio, Dalian, China) assay. Cells were inoculated in 96-well plates at a density of 1×10^4 cells per well. Cells were treated with Genipin for 48 hours, followed by CCK-8 solution at 37°C for 3 hours. The absorbance at 595 nm was measured using an enzyme marker

(SPECTRA190, Molecular Devices, Sunnydale, CA, USA).

3.1.12 Colony formation assay

Cells were inoculated at a low density of approximately 1×10^3 cells per well into 6-well plates lined with methylcellulose. Cells were cultured for 7 days. Photographs were taken under an inverted microscope lens.

3.1.13 Apoptosis analysis (flow cytometry)

Cells were untreated or treated with Genipin for 48 hours. With 5 μL Annexin V-fluorescein isothiocyanate reagent and 10 μL 7-Aminoactinomycin D (7-AAD) reagent for 30 min at room temperature and protected from light. Cells were analyzed by flow cytometry (Beckman Coulter, Brea, CA, USA) immediately after termination of staining.

3.1.14 Cell cycle analysis

For cell cycle assays, cells were treated with Genipin for 48 hours. Cells were then stained with propidium iodide at a final concentration of 0.05 mg/mL and incubated at 4°C for 20 minutes in the dark. Data were collected and analyzed using flow cytometry.

3.1.15 Incorporation of mitochondrial reactive oxygen species (ROS)

HL-60, Kasumi-1 cells were inoculated in 6-well plates and treated with Genipin for 6 hours. After incubation with MitoSOX (Thermo Fisher Scientific) at 37 °C for 30 min, cells were collected by centrifugation and analyzed for mitochondrial ROS using flow

cytometry.

3.1.16 Statistical analysis

All RNA-seq expression data were log_2 normalized for further analysis. At the same time, some of the figures are made by the SangerBox Website (http://sangerbox.com)(14). Results with p-values less than 0.05 were considered significantly different. R (version 3.6.1) and GraphPad Prism (version 8.0.1) were used for statistical analysis.

3.2 Results

3.2.1 Identification Analysis of OS-Related ARGs in AML

Univariate COX proportional risk regression analysis was used to screen for ARGs with P values less than 0.05 to help identify potential ARGs associated with AML prognosis. The expression of 75 of these AGRs in AML patients was considered to be meaningfully correlated with OS (Figure 1A). To further improve the precision and reduce the number of genes, we integrated the survival time and survival status of AML patients, together with the ARGs expression data, and performed regression analysis using the LASSO-Cox method. We finally took the lambda minimum value:0.136228890858806 and screened out 12 genes (Figures 1B, C).

The model equation constructed was: RiskScore =0.278283555346816* *AIFM1* - 0.0475492647482181* *DLL3* -0.0014067701404597* *GDF11* +0.0542005253161292* *GH1* - 0.195140667960413* *HBP1* -0.0498890983609883*

INSR +0.243526421013745* *PTPN1* +0.0251203847594925* *SOCS2* +0.0864246729795927* *TERF2* + 0.0656487992927026* *TGFB1* - 0.167371227915521* *TPP2* +0.18031172128784* *UCP2*

3.2.2 Validation of ARG-related prognostic features in the training set

AML patients were divided into two groups, high-and low-risk, by median risk score. Kaplan–Meier survival analysis demonstrated significant differences in OS between the two groups (Figure 1D). Next, we used time-dependent ROC curves to assess the predictive efficacy for different time points in the training set (Figure 1F). the AUC values at 1, 3, and 5 years were 0.82, 0.83, and 0.90 (Figure 1F). Respectively, they indicated that the predictive efficacy of the feature was high. As the risk score increased in the high-risk versus low-risk group, the survival time decreased gradually in both groups. The expression profile heat map of the 12 ARGs is shown in Figure x. In the high-risk group, *AIFM1, PTPN1, SOCS2, TERF2, TGFB1, UCP2*, and *GH1* were highly expressed, while *DLL3, GDF11, HBP1, INSR*, and *TPP2* in the low-risk group expression was higher (Figure 1E).

3.2.3 Patients at different risks showed different immune status

Next, this study further explored the differences in immune status between patients in different risk groups. First, the CIBERSORT algorithm was used to assess the percentage of immune cell types in each patient. The results show the percentage of immune cells in AML patients in the low-risk group versus the high-risk group (Figure 2A). In particular, patients in the high-risk group had elevated proportions of T-cells-

regulatory-(Tregs), NK-cells-activated, and Monocytes, while the low-risk group showed higher proportions of T-cells-CD4-memory-resting, Macrophages-M0 Dendritic-cells-activated, and Mast-cells-resting (Figure 2B). The figure below also shows the correlation between different types of immune cells (Figure 2C). Subsequently, the ESTIMATE algorithm was used to assess the immune differences between the two groups of patients with different risks. The results showed that patients in the high-risk group had higher immune scores, stromal scores as well as assessment scores, and lower tumor purity compared to the low-risk group (Figure 2D). In addition, the EPIC score was also used to assess immune differences, and the results showed a higher proportion of B-cells, Endothelial, and Macrophages, and a lower proportion of Other cells in the high-risk group compared to the low-risk group, with no significant differences in other types of immune cells (Figures 2E, F).

3.2.4 DEG and Functional Analyses

The genes were grouped according to high- and low-risk, and differentiated genes were identified. A total of 906 differential genes were screened, of which 578 genes were up-regulated and 328 genes were down-regulated in the high-risk group compared to the low-risk group (Figure 3A). Figure 3B shows the Protein-Protein Interaction (PPI) Networks between differential genes. GO gene enrichment analysis showed that DEGs were mostly enriched in biological processes such as the immune system process, immune response, and cell activation (Figure 3C). In terms of cellular components, DEGs were mainly enriched in the vesicle, cytoplasmic vesicle part, cytoplasmic

vesicle, and intracellular vesicle (Figure 3D). Meanwhile, In molecular functions, DEGs mainly showed cytokine binding, cargo receptor activity, and peptide binding (Figure 3E). In the KEGG enrichment analysis, DEGs were mainly enriched in the pathways of Phagosome, Hematopoietic cell lineage, Tuberculosis, Staphylococcus aureus infection, and Rheumatoid arthritis (Figure 3F).

On this basis, GSEA was used to obtain the enrichment of DEGs in different pathways in this study, and the results showed that the high risk was mainly associated with ALZHEIMERS DISEASE (NES=2.0537, NP=0.0081), VIRAL MYOCARDITIS (NES=2.0457, NP=0.0020), ANTIGEN PROCESSING AND PRESENTATION (NES=2.0617, NP=0.0020), VASOPRESSIN REGULATED WATER REABSORPTION (NES=1.9877, NP=0.0020), APOPTOSIS (NES= 2.0676, NP=0.0020), ADIPOCYTOKINE SIGNALING PATHWAY (NES=1.9919, NP=0.0021), B CELL RECEPTOR SIGNALING PATHWAY (NES=2.1087, NP=0.0020), NATURAL KILLER CELLMEDIATEDCYTOTOXICITY (NES=2.0052, NP=0.0040) pathways were associated (Figure 3G). These results demonstrate that are mainly associated with immune-related pathways.

3.2.5 Validation of ARG-related prognostic features in an external dataset

To further validate the predictive efficacy of ARG-related prognostic features in the external dataset. The risk scores of different datasets (GSE12417, GSE71014) were calculated according to the feature formula. To calculate the optimal cut-off value of the risk score, patients were divided into two cohorts. In the GSE12417 cohort, OS

showed differences between the high- and low-risk groups, with an AUC value of 0.61 for 1-year OS and 0.53 for 3-year AUC in this cohort (Figure 4A, B); meanwhile, the high-risk group in the GSE71014 set had worse OS than the low-risk group, with a 1-year AUC of 0.58 and a 3-year AUC of 0.55 (Figures 4C, D). The above suggests that this feature can be used to predict the prognosis of AML patients.

3.2.6 UCP2 expression levels are elevated in AML patients

We selected bone marrow samples from four healthy individuals and five AML patients and examined their gene expression. Subsequently, the experiment showed that AML patients expressed higher *UCP2* in bone marrow compared to healthy individuals (Figure 4E). And the expression levels of UCP2 also differed in different cell lines. (Figure 4F)

3.2.7 UCP2 pan-cancer immunoassay

Subsequently, this study calculated the difference in expression between normal and tumor samples in each tumor in the TCGA database and performed differential significance analysis 24 tumors were observed to be significantly upregulated as shown in Figure 5A and significant downregulation was observed in 3 tumors. Subsequently, Cox, proportional hazards regression mode was used to analyzing the prognostic relationship between *UCP2* expression and various tumors, and finally, it was observed that high expression in TCGA-LAML (N=209, p=2.7e-4, HR=1.47(1.20,1.81)) in 7 tumor types had a poor prognosis, and low expression in 5 tumor types had a poor prognosis. The prognosis was poor for low expression in five tumor types (Figure 5B).

We next calculated the Pearson correlation between ENSG00000175567 (*UCP2*) and marker genes of the five types of immune pathways as shown in Figure 5C. Obtaining DNAss tumor stemness scores calculated by methylation profiles in each tumor and calculating their Pearson correlation, we observed significant correlations in 16 tumors, including in 11 tumors significant positive correlations and in 5 tumors significant negative correlations (Figure 5D).

3.2.8 Genipin can effectively inhibit cellular activity *in vitro*

To further investigate the role of *UCP2* in AML, we selected Genipin as a protein inhibitor. It inhibits UCP2 in cells. It is now often used in studies of type 2 diabetes and has been reported to act in breast cancer cells in oncology. To clarify whether Genipin kills AML cells, two common AML cell lines (Kasumi-1, HL-60) were used in this study, and cell proliferation activity was assayed after 48 hours of treatment with Genipin. The results showed that Genipin inhibited the proliferative activity of AML cells in a dose-dependent manner (Figure 6A). Afterward, the proliferative passaging ability of Genipin-treated cells was assessed by colony formation assay, as shown in Figures 6B, C. Genipin treatment at 200 μM significantly reduced the number of colony formation of AML cells on day 7.

3.2.9 Genipin blocks the AML cell cycle *in vitro* and promotes apoptosis

Cell cycle distribution plays a significant role in cell growth and proliferation, and the cell cycle distribution of each group was examined by flow cytometry after treatment of different cell lines with different concentrations of Genipin for 48 hours. As shown

in Figure 6C, in the HL-60 and Kasumi-1 cell line, Genipin significantly increased the proportion of G2 phase cells compared to the control, while the proportion of G1 phase cells was not reduced or slightly reduced, and the proportion of S-phase cells also decreased gradually with Genipin dose (Figure 6D, E). These data suggest that Genipin may stunt the proliferation of AML cells by altering their cycle. Next, to investigate whether Genipin can cause apoptosis while reducing cell viability, this study also used flow cytometry to examine the number of Annexin V/7AAD-stained cells. The results showed that in both cell lines, apoptotic cells gradually increased with increasing doses of Genipin after 48 hours of treatment. It indicates that Genipin can increase AML cell apoptosis in a dose-dependent manner (Figure 7A).

3.2.10 Genipin affects the level of reactive oxygen species in AML cells

Reactive oxygen species (ROS) levels in cells are thought to be associated with cellular activity, and in this study, a dose-dependent decrease in ROS levels was found in the HL-60 cell line 6 hours after Genipin treatment (Figure 7B). In contrast, the Kasumi-1 cell line did not show significant changes in ROS levels, suggesting that UCP2 may not affect cellular activity by altering its ROS levels. The above suggests that Genipin may affect the cellular activity of some AML cell lines by altering their reactive oxygen species levels.

3.3 Discussion

AML is the most common neoplastic disease of the hematologic system, and despite the many studies and results available, the prognosis for patients with AML remains

poor. Worse, although most patients improve with treatment, a significant number of patients eventually relapse, which contributes to the low survival rate of AML. In recent years, there has been a lot of interest in predictive models for predicting the prognosis of AML(15, 16). While the role of ARGs in AML and their potential mechanisms are still not elucidated, this study constructed and validated ARG risk models and predicted their potential impact on the prognosis of AML patients. And we discovered that Genipin, a drug that inhibits UCP2 protein, can kill AML cells *in vitro*.

Certain injuries or physiological processes that lead to prolongation or blockage of the cell cycle are called cellular senescence. Cellular senescence is found in different tumors because of its anti-proliferative effect and is also considered a new anti-tumor mechanism and has the potential to develop novel therapies accordingly. Cellular senescence is also frequently mentioned in AML, and it has been shown that senescence-related factors can regulate the transition from acquired aplastic anemia (AA) and paroxysmal nocturnal hemoglobinuria (PNH) to secondary myelodysplastic syndromes (MDS) and AML(17). Genetic targets commonly used to treat leukemia, such as *BCL-2* and *P53*, can also act by regulating cellular senescence(18, 19).

The immune microenvironment is present in various tumors and is strongly associated with tumor prognosis(20), while cellular senescence is also present in the bone marrow immune microenvironment, and it has been shown that T cell senescence and prognosis can be used to predict the prognosis of patients with AML(21), which has important roles in inducing drug resistance and mediating immune escape(22, 23). Another study showed that a higher proportion of Tregs in AML patients compared to healthy donors

can also affect AML prognosis(24, 25). Activated NK cells kill cancer cells, and there and various related products are currently used to adjuvantly target cancer therapy(26-28). Resting $CD4^+$ T cells, and resting mast cells are associated with tumor cell killing. In contrast, activated dendritic cells activate T cells in the tumor microenvironment and modulate the immune response. Macrophages also play an important role in the tumor microenvironment, and our study shows that the tumor microenvironment differs significantly between high- and low-risk groups, suggesting that immunotherapy remains largely unexplored and may become a new therapeutic tool(29, 30).

UCP2 belongs to the family of mitochondrial anion carrier proteins located on the inner mitochondrial membrane(31). Many reports have shown that it can induce adaptive responses to prevent oxidative stress(32). Tumor cells attenuate the toxic effects of ROS by regulating the expression of *UCP2*, which leads to an increase in their proliferation(33). A recent study showed that AML cells exhibit high ROS levels and regulate *UCP2* expression upregulation(34). ROS are mainly produced by mitochondria to maintain redox homeostasis in the body, and ROS are not only essential for the normal organism but also play a key role in tumors. A strong association between ROS and AML cell proliferation has been reported in the literature(35). And either too high or too low ROS affects AML cell proliferation(36, 37). In this study, *UCP2* levels were found to be closely associated with the prognosis of AML. Genipin is a specific UCP2 inhibitor that is derived from plants(38). Its mechanism of action has been recently explained(39, 40). We used Genipin to act on AML cell lines *in vitro*. In this study, *in vitro* experiments showed that Genipin induces antitumor activity

against AML by inhibiting cell proliferation and cell cycle, while also inducing apoptosis and scavenging high ROS levels in AML. This suggests that drugs targeting UCP2 protein, especially Genipin, may become new targets for the treatment of AML.

4. Declaration

Acknowledgements

The authors declare that the research was conducted in the absence of any commercial or financial relationships that could be construed as a potential conflict of interest.

Funding

This work was supported by the major project of the Wenzhou Municipal Science and Technology Bureau (No. ZY2012013).

Availability of data and material

The datasets generated during and analyses during the current study are available in the The Cancer Genome Atlas (TCGA) and Gene Expression Omnibus (GEO).

Ethics approval and consent to participate

The experimental protocol was established, according to the ethical guidelines of the Helsinki Declaration and was approved by the Human Ethics Committee of The First Affiliated Hospital of Wenzhou Medical University (2017-044).

Competing interests

The authors declare that the research was conducted in the absence of any commercial or financial relationships that could be construed as a potential conflict of interest.

Consent for publication

Not applicable.

Authors' contributions

Dongxu Gang: Conceptualization, Methodology, Writing - Original Draft. **Yinyan Jiang**: Conceptualization, Methodology, Writing - Original Draft. **Xiaofang Wang**: Formal analysis, Investigation. **Jifan Zhou**: Data Curation, Visualization. **Xiaoyuan Zhang**: Methodology, Visualization. **Xiaoyu He**: Formal analysis, Investigation. **Rujiao Dong**: Data Curation, Writing - Original Draft. **Ziyang Huang**: Writing - Review & Editing, Supervision. **Songfu Jiang**: Project administration, Funding acquisition, Writing - Review & Editing.

Author details

[1]Department of Hematology, The First Affiliated Hospital of Wenzhou Medical University, Southern white elephant Wenzhou325000, Zhejiang, China.

5 References

1. Shallis RM, Wang R, Davidoff A, Ma X, Zeidan AM. Epidemiology of acute myeloid leukemia: Recent progress and enduring challenges. Blood Rev. 2019;36:70-87.

2. Papaemmanuil E, Gerstung M, Bullinger L, Gaidzik VI, Paschka P, Roberts ND, et al. Genomic Classification and Prognosis in Acute Myeloid Leukemia. New Engl J Med. 2016;374(23):2209-21.

3. Li F, Cai J, Liu J, Yu SC, Zhang X, Su Y, et al. Construction of a solid Cox model for AML patients based on multi-omics bioinformatic analysis. Front Oncol. 2022;12:925615.

4. Gorgoulis V, Adams PD, Alimonti A, Bennett DC, Bischof O, Bishop C, et al. Cellular

415 Senescence: Defining a Path Forward. Cell. 2019;179(4):813-27.

416 5. Lee S, Schmitt CA. The dynamic nature of senescence in cancer. Nat Cell Biol. 2019;21(1):94-

417 101.

418 6. Galanos P, Vougas K, Walter D, Polyzos A, Maya-Mendoza A, Haagensen EJ, et al. Chronic

419 p53-independent p21 expression causes genomic instability by deregulating replication licensing.

420 Nat Cell Biol. 2016;18(7):777-89.

421 7. Coppe JP, Desprez PY, Krtolica A, Campisi J. The senescence-associated secretory phenotype:

422 the dark side of tumor suppression. Annu Rev Pathol. 2010;5:99-118.

423 8. Xu Q, Chen Y. An Aging-Related Gene Signature-Based Model for Risk Stratification and

424 Prognosis Prediction in Lung Adenocarcinoma. Front Cell Dev Biol. 2021;9:685379.

425 9. Jin S, Kim JG, Park JW, Koch M, Horvath TL, Lee BJ. Hypothalamic TLR2 triggers sickness

426 behavior via a microglia-neuronal axis. Sci Rep. 2016;6:29424.

427 10. Liu YG, Dai QL, Wang SB, Deng QJ, Wu WG, Chen AZ. Preparation and in vitro antitumor

428 effects of cytosine arabinoside-loaded genipin-poly-l-glutamic acid-modified bacterial

429 magnetosomes. Int J Nanomedicine. 2015;10:1387-97.

430 11. Yao ML, Gu J, Zhang YC, Wang N, Zhu ZH, Yang QT, et al. [Inhibitory effect of Genipin on

431 uncoupling protein-2 and energy metabolism of androgen-independent prostate cancer cells].

432 Zhonghua Nan Ke Xue. 2015;21(11):973-6.

433 12. Youngren-Ortiz SR, Hill DB, Hoffmann PR, Morris KR, Barrett EG, Forest MG, et al.

434 Development of Optimized, Inhalable, Gemcitabine-Loaded Gelatin Nanocarriers for Lung Cancer.

435 J Aerosol Med Pulm Drug Deliv. 2017;30(5):299-321.

436 13. Hu J, Yu A, Othmane B, Qiu D, Li H, Li C, et al. Siglec15 shapes a non-inflamed tumor

437 microenvironment and predicts the molecular subtype in bladder cancer. Theranostics.
438 2021;11(7):3089-108.
439 14. Shen W, Song Z, Zhong X, Huang M, Shen D, Gao P, et al. Sangerbox: A comprehensive,
440 interaction-friendly clinical bioinformatics analysis platform. iMeta. 2022;1(3):e36.
441 15. Fu D, Zhang B, Wu S, Zhang Y, Xie J, Ning W, et al. Prognosis and Characterization of Immune
442 Microenvironment in Acute Myeloid Leukemia Through Identification of an Autophagy-Related
443 Signature. Front Immunol. 2021;12:695865.
444 16. Zheng PF, Zou QC, Chen LZ, Liu P, Liu ZY, Pan HW. Identifying patterns of immune related
445 cells and genes in the peripheral blood of acute myocardial infarction patients using a small cohort.
446 J Transl Med. 2022;20(1):321.
447 17. Sun L, Babushok DV. Secondary myelodysplastic syndrome and leukemia in acquired aplastic
448 anemia and paroxysmal nocturnal hemoglobinuria. Blood. 2020;136(1):36-49.
449 18. Yosef R, Pilpel N, Tokarsky-Amiel R, Biran A, Ovadya Y, Cohen S, et al. Directed elimination
450 of senescent cells by inhibition of BCL-W and BCL-XL. Nat Commun. 2016;7:11190.
451 19. Baker DJ, Wijshake T, Tchkonia T, LeBrasseur NK, Childs BG, van de Sluis B, et al. Clearance of
452 p16Ink4a-positive senescent cells delays ageing-associated disorders. Nature.
453 2011;479(7372):232-6.
454 20. Wang Y, Wang Y, Xu C, Liu Y, Huang Z. Identification of Novel Tumor-Microenvironment-
455 Regulating Factor That Facilitates Tumor Immune Infiltration in Colon Cancer. Mol Ther Nucleic
456 Acids. 2020;22:236-50.
457 21. Tang L, Wu J, Li CG, Jiang HW, Xu M, Du M, et al. Characterization of Immune Dysfunction
458 and Identification of Prognostic Immune-Related Risk Factors in Acute Myeloid Leukemia. Clin

459 Cancer Res. 2020;26(7):1763-72.

460 22. Sallman DA, McLemore AF, Aldrich AL, Komrokji RS, McGraw KL, Dhawan A, et al. TP53

461 mutations in myelodysplastic syndromes and secondary AML confer an immunosuppressive

462 phenotype. Blood. 2020;136(24):2812-23.

463 23. Tettamanti S, Pievani A, Biondi A, Dotti G, Serafini M. Catch me if you can: how AML and its

464 niche escape immunotherapy. Leukemia. 2022;36(1):13-22.

465 24. Williams P, Basu S, Garcia-Manero G, Hourigan CS, Oetjen KA, Cortes JE, et al. The distribution

466 of T-cell subsets and the expression of immune checkpoint receptors and ligands in patients with

467 newly diagnosed and relapsed acute myeloid leukemia. Cancer. 2019;125(9):1470-81.

468 25. Dama P, Tang M, Fulton N, Kline J, Liu H. Gal9/Tim-3 expression level is higher in AML patients

469 who fail chemotherapy. J Immunother Cancer. 2019;7(1):175.

470 26. Myers JA, Miller JS. Exploring the NK cell platform for cancer immunotherapy. Nat Rev Clin

471 Oncol. 2021;18(2):85-100.

472 27. Szaflarska A, Baj-Krzyworzeka M, Siedlar M, Weglarczyk K, Ruggiero I, Hajto B, et al.

473 Antitumor response of CD14+/CD16+ monocyte subpopulation. Exp Hematol. 2004;32(8):748-55.

474 28. Headley MB, Bins A, Nip A, Roberts EW, Looney MR, Gerard A, et al. Visualization of

475 immediate immune responses to pioneer metastatic cells in the lung. Nature. 2016;531(7595):513-

476 7.

477 29. Xiao W, Chan A, Waarts MR, Mishra T, Liu Y, Cai SF, et al. Plasmacytoid dendritic cell expansion

478 defines a distinct subset of RUNX1-mutated acute myeloid leukemia. Blood. 2021;137(10):1377-

479 91.

480 30. Chao MP, Takimoto CH, Feng DD, McKenna K, Gip P, Liu J, et al. Therapeutic Targeting of the

481 Macrophage Immune Checkpoint CD47 in Myeloid Malignancies. Front Oncol. 2019;9:1380.
482 31. Echtay KS, Roussel D, St-Pierre J, Jekabsons MB, Cadenas S, Stuart JA, et al. Superoxide
483 activates mitochondrial uncoupling proteins. Nature. 2002;415(6867):96-9.
484 32. Donadelli M, Dando I, Fiorini C, Palmieri M. UCP2, a mitochondrial protein regulated at
485 multiple levels. Cell Mol Life Sci. 2014;71(7):1171-90.
486 33. Ji R, Chen W, Wang Y, Gong F, Huang S, Zhong M, et al. The Warburg Effect Promotes
487 Mitochondrial Injury Regulated by Uncoupling Protein-2 in Septic Acute Kidney Injury. Shock.
488 2021;55(5):640-8.
489 34. He H, Wang C, Liu G, Ma H, Jiang M, Li P, et al. Isobavachalcone inhibits acute myeloid
490 leukemia: Potential role for ROS-dependent mitochondrial apoptosis and differentiation.
491 Phytother Res. 2021;35(6):3337-50.
492 35. Zhou R, Tardivel A, Thorens B, Choi I, Tschopp J. Thioredoxin-interacting protein links
493 oxidative stress to inflammasome activation. Nat Immunol. 2010;11(2):136-40.
494 36. Prasad S, Gupta SC, Tyagi AK. Reactive oxygen species (ROS) and cancer: Role of antioxidative
495 nutraceuticals. Cancer Lett. 2017;387:95-105.
496 37. Hole PS, Zabkiewicz J, Munje C, Newton Z, Pearn L, White P, et al. Overproduction of NOX-
497 derived ROS in AML promotes proliferation and is associated with defective oxidative stress
498 signaling. Blood. 2013;122(19):3322-30.
499 38. Cho YS. Genipin, an Inhibitor of UCP2 as a Promising New Anticancer Agent: A Review of the
500 Literature. Int J Mol Sci. 2022;23(10).
501 39. Muzzarelli RA, El Mehtedi M, Bottegoni C, Aquili A, Gigante A. Genipin-Crosslinked Chitosan
502 Gels and Scaffolds for Tissue Engineering and Regeneration of Cartilage and Bone. Mar Drugs.

2015;13(12):7314-38.

40. Wei M, Wu Y, Liu H, Xie C. Genipin Induces Autophagy and Suppresses Cell Growth of Oral Squamous Cell Carcinoma via PI3K/AKT/MTOR Pathway. Drug Des Devel Ther. 2020;14:395-405.

6 Figures

Figure 1. Identification Analysis of OS-Related ARGs in AML and Validation of ARG-related prognostic features in the training set

(A) Prognosis-related genes that overlap between TCGA and ARGs.

(B) Selection of optimal parameters (lambda) in the least absolute shrinkage and selection operator (LASSO) model; dashed vertical lines are drawn at the optimal values using the minimum criterion.

(C) LASSO coefficient curves for 75 prognosis-related ARGs with nonzero coefficients determined by the optimal lambda.

(D) Overall survival curves stratified by the low- and high-risk group.

(E) Distribution of risk scores calculated from risk scores. and the distribution of patients in low- and high-risk fractional groups based on survival status. A heat map of the ARGs expression chart is shown below.

(F) ROC curves for ARG-based overall survival prediction.

Figure 2. Patients at different risks showed different immune status

(A) Immune cell type percentages in the low- and high-risk groups.

(B) Differences in the abundance of immune cells between the high- and low-risk groups.

(C) Correlation matrix of immune infiltrating cells.

(D) stromal score, immune score, ESTIMATE score, and tumor purity calculated by ESTIMATE algorithm

(E) the abundance of six immune filtrating cells evaluated by EPIC

(F) EPIC assesses immune cell type differences in low and high-risk groups.

Figure 3. DEGs and Functional Analyses

(A) Volcano plot showing the DEGs between the two risk groups.

(B) PPI of differential genes between the two groups.

(C)(D)(E) GO gene enrichment analysis of differential genes in (C)BP,(D)CC, and **(E)** MF enrichment results.

(F) KEGG gene enrichment analysis of differential genes.

(G) Major pathways of biological significance in GSEA, ranked by NES.

Figure 4. Validation of ARG-related prognostic features in an external dataset and finding that *UCP2* expression levels are elevated in AML patients

(A)(B) Overall survival curves by low- and high-risk groups for the (A)GSE12417, and (C)GSE71014 datasets.

(B)(D) ROC curve plot based on ARGs of patients in validation dataset (B) GSE12417,

(D) GSE71014.

(E) Differences in the relative expression levels of *UCP2* between healthy individuals and patients with newly diagnosed AML.

(F) Differences of the relative expression levels of *UCP2* in four cell lines.

Figure 5. *UCP2* pan-cancer immunoassay

(A) Differential expression of *UCP2* in multiple tumors.

(B) Prognostic relevance of *UCP2* in multiple tumors.

(C) Pearson correlation between *UCP2* and marker genes of five types of immune pathways.

(D) Correlation between tumor stemness and *UCP2* expression.

Figure 6. Genipin can effectively inhibit cellular activity *in vitro* and Genipin blocks the AML cell cycle *in vitro*

(A) The effect of Genipin on the viability of HL-60, and Kasumi-1 cells was measured by CCK-8 assay.

(B)(C) A colony formation assay was performed to examine the effect of Genipin on the proliferation of HL60, and Kasumi-1 cells.

(D)(E) Flow cytometry assay of the effect of Genipin on HL-60, Kasumi-1 cell cycle.

Figure 7. Genipin reduces the level of reactive oxygen species in AML cells and promotes apoptosis.

(A) Flow cytometric detection of the effect of Genipin on the apoptosis of HL-60, Kasumi-1 cells.

(B) Flow cytometry was performed to detect intracellular ROS levels in HL-60, Kasumi-1 cells after 6 hours of Genipin treatment.

Figures

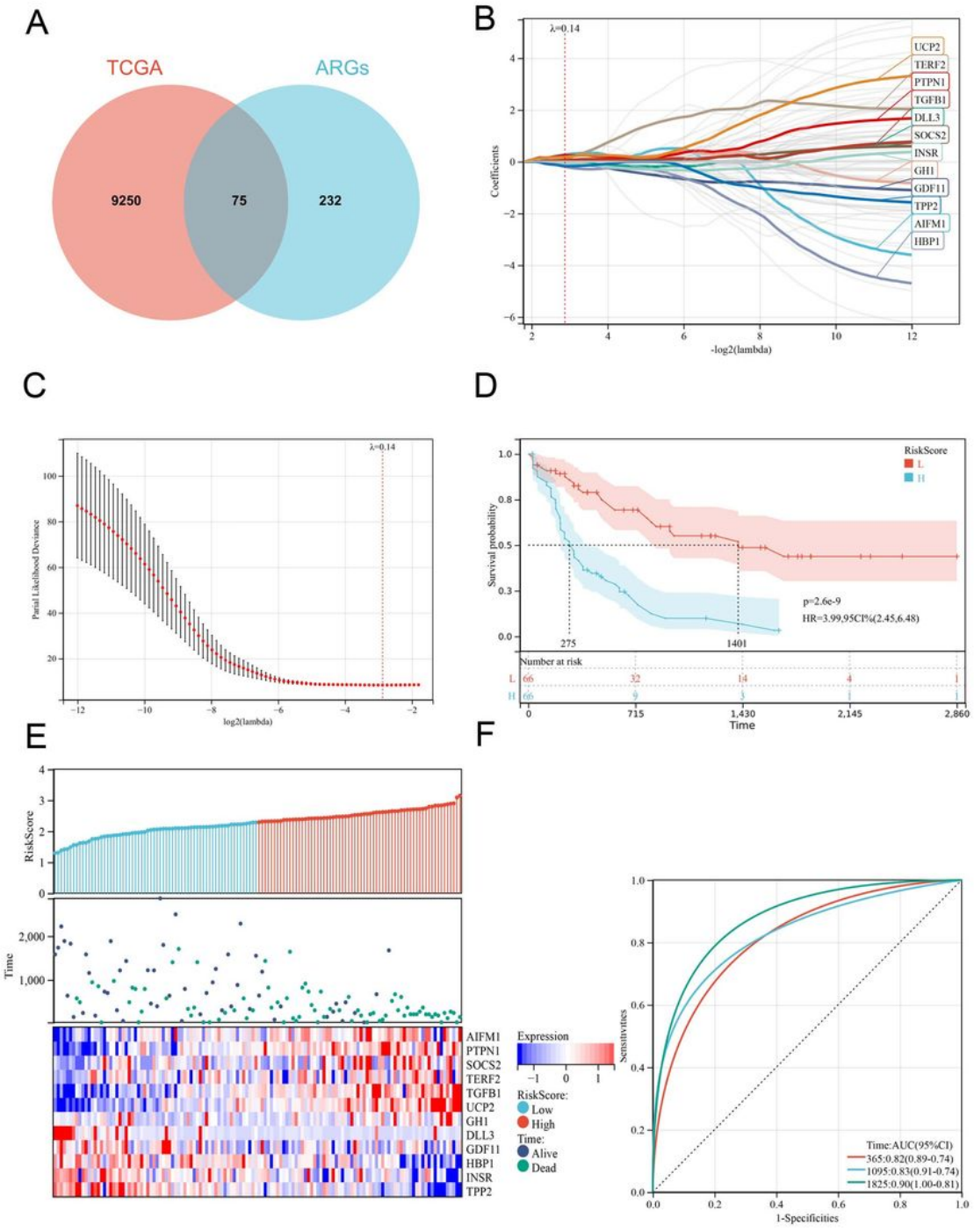

Figure 1

Identification Analysis of OS-Related ARGs in AML and Validation of ARG-related prognostic features in the training set

(A) Prognosis-related genes that overlap between TCGA and ARGs.

(B) Selection of optimal parameters (lambda) in the least absolute shrinkage and selection operator (LASSO) model; dashed vertical lines are drawn at the optimal values using the minimum criterion.

(C) LASSO coefficient curves for 75 prognosis-related ARGs with nonzero coefficients determined by the optimal lambda.

(D) Overall survival curves stratified by the low- and high-risk group.

(E) Distribution of risk scores calculated from risk scores. and the distribution of patients in low- and high-risk fractional groups based on survival status. A heat map of the ARGs expression chart is shown below.

(F) ROC curves for ARG-based overall survival prediction.

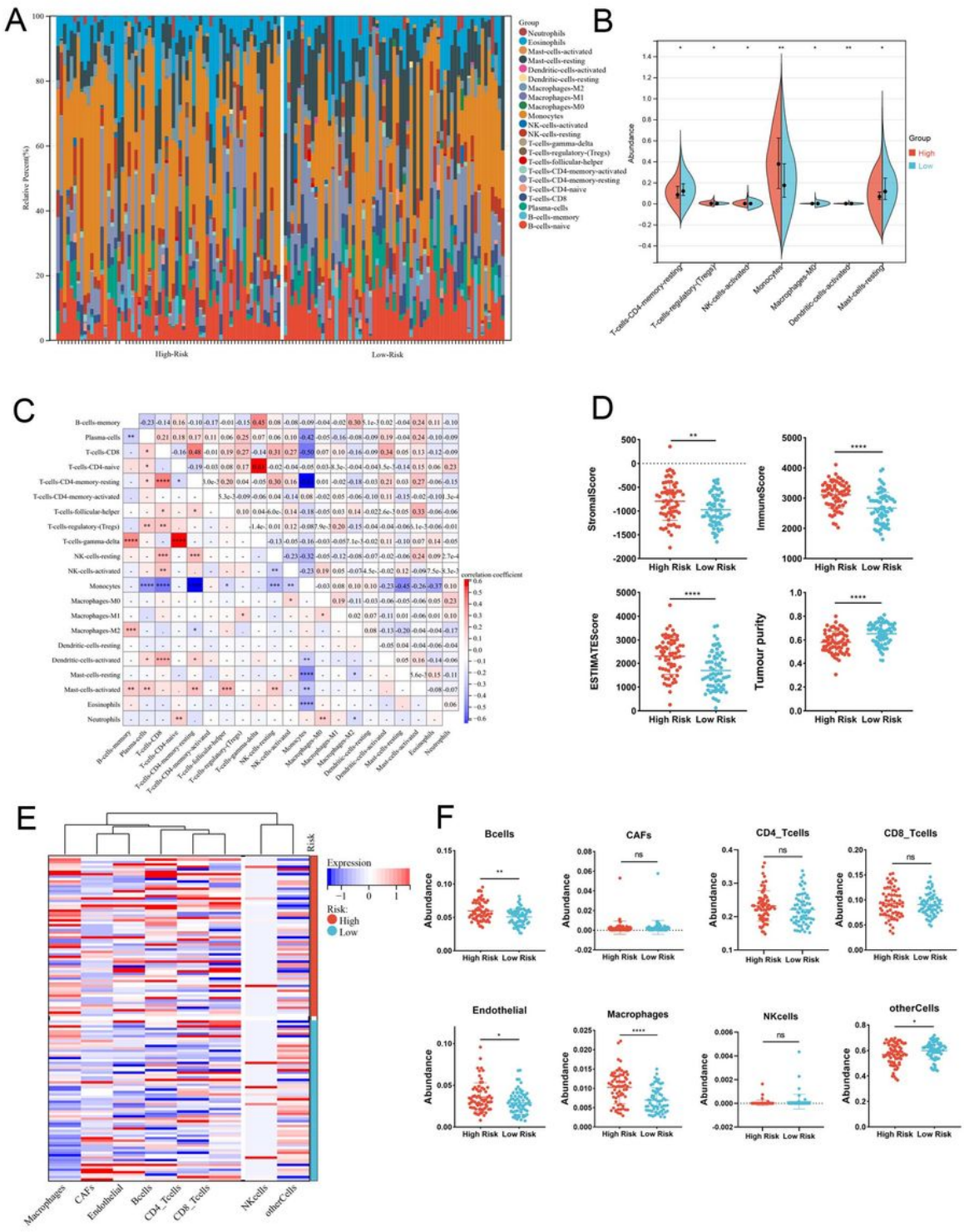

Figure 2

Patients at different risks showed different immune status

(A) Immune cell type percentages in the low- and high-risk groups.

(B) Differences in the abundance of immune cells between the high- and low-risk groups.

(C) Correlation matrix of immune infiltrating cells.

(D) stromal score, immune score, ESTIMATE score, and tumor purity calculated by ESTIMATE algorithm

(E) the abundance of six immune filtrating cells evaluated by EPIC

(F) EPIC assesses immune cell type differences in low and high-risk groups.

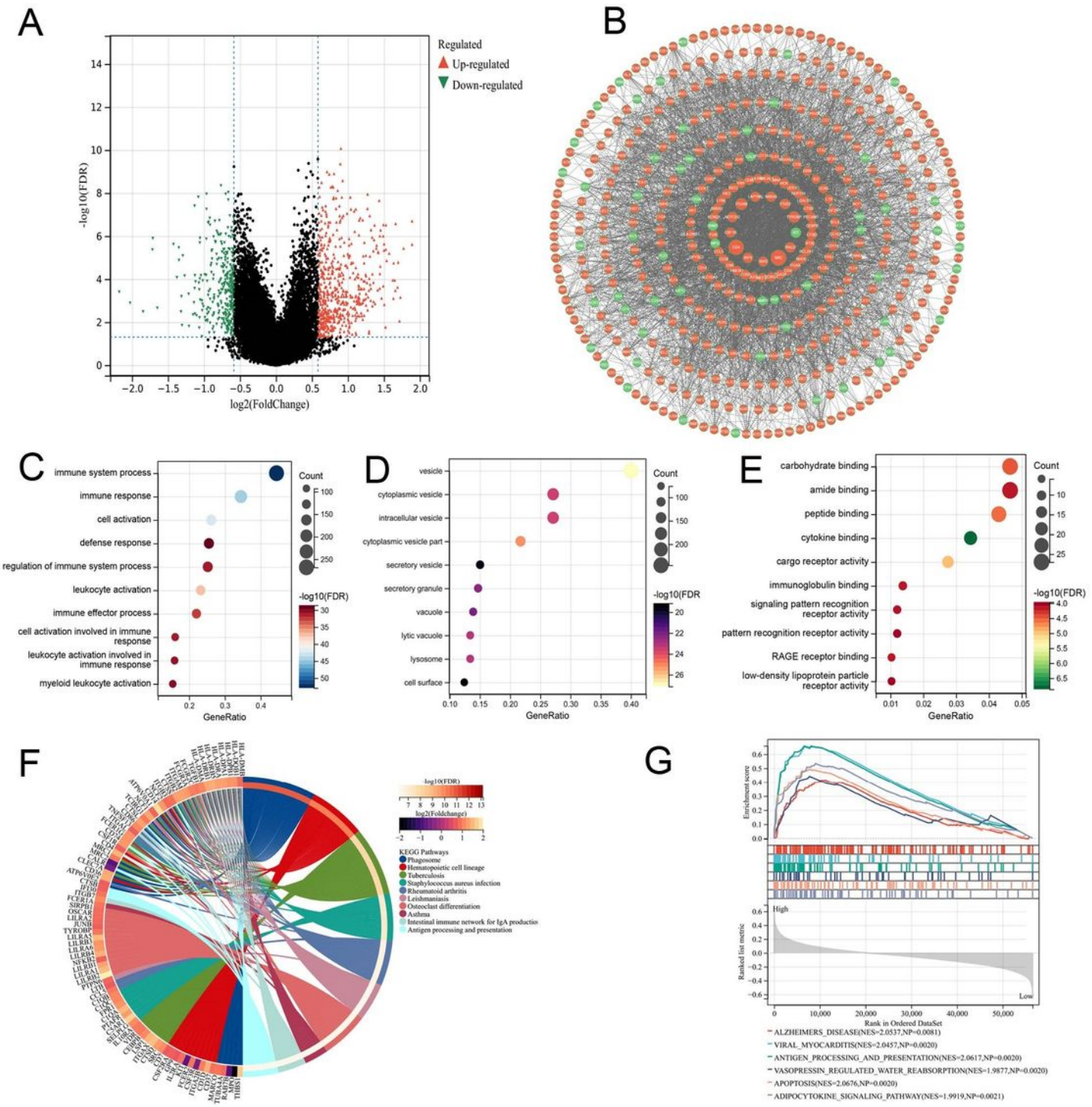

Figure 3

DEGs and Functional Analyses

(A) Volcano plot showing the DEGs between the two risk groups.

(B) PPI of differential genes between the two groups.

(C)(D)(E) GO gene enrichment analysis of differential genes in (C)BP,(D)CC, and (E) MF enrichment results.

(F) KEGG gene enrichment analysis of differential genes.

(G) Major pathways of biological significance in GSEA, ranked by NES.

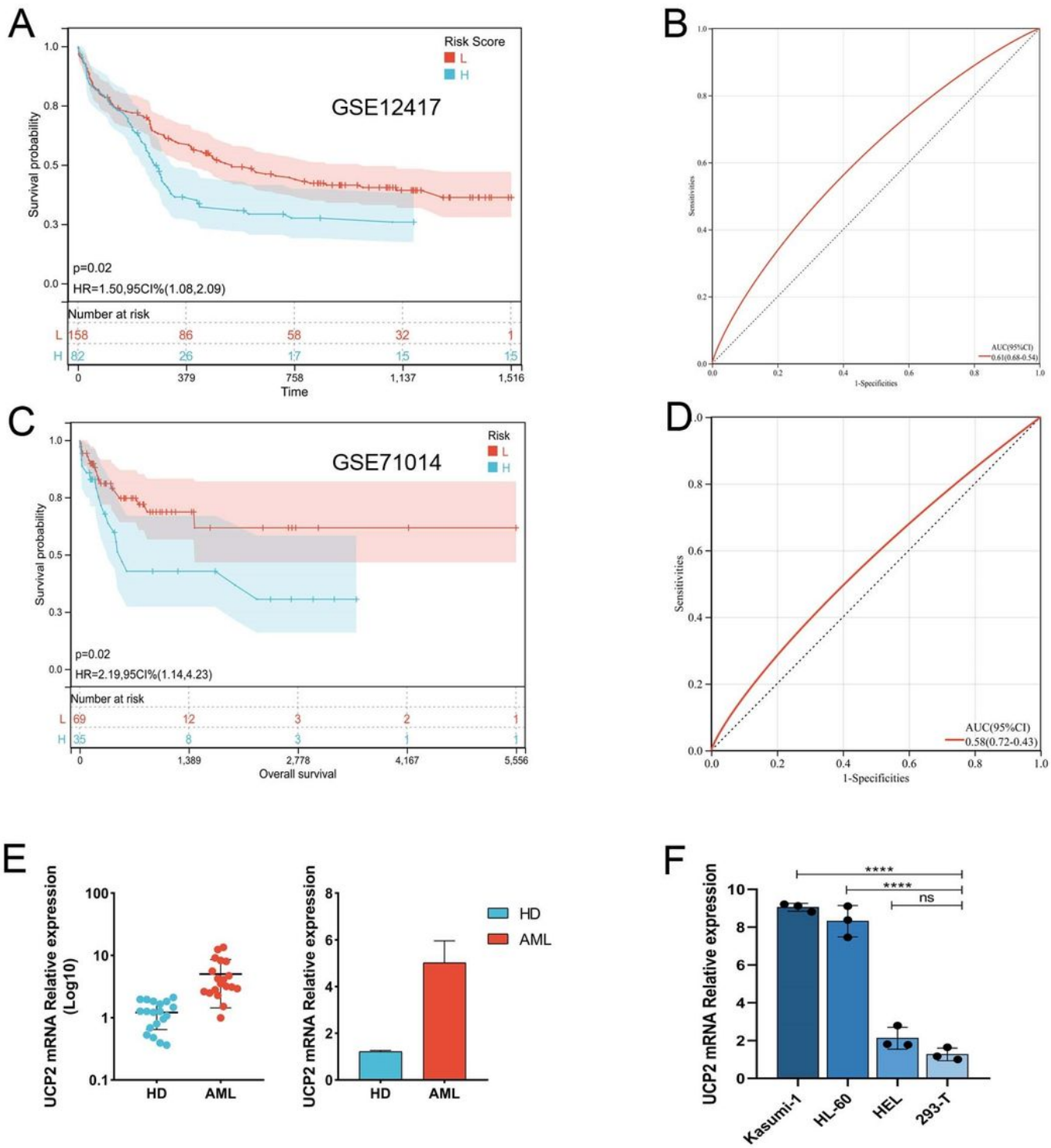

Figure 4

Validation of ARG-related prognostic features in an external dataset and finding that UCP2 expression levels are elevated in AML patients

(A)(B) Overall survival curves by low- and high-risk groups for the (A)GSE12417, and (C)GSE71014 datasets.

(B)(D) ROC curve plot based on ARGs of patients in validation dataset (B) GSE12417,

(D) GSE71014.

(E) Differences in the relative expression levels of UCP2 between healthy individuals and patients with newly diagnosed AML.

(F) Differences of the relative expression levels of UCP2 in four cell lines.

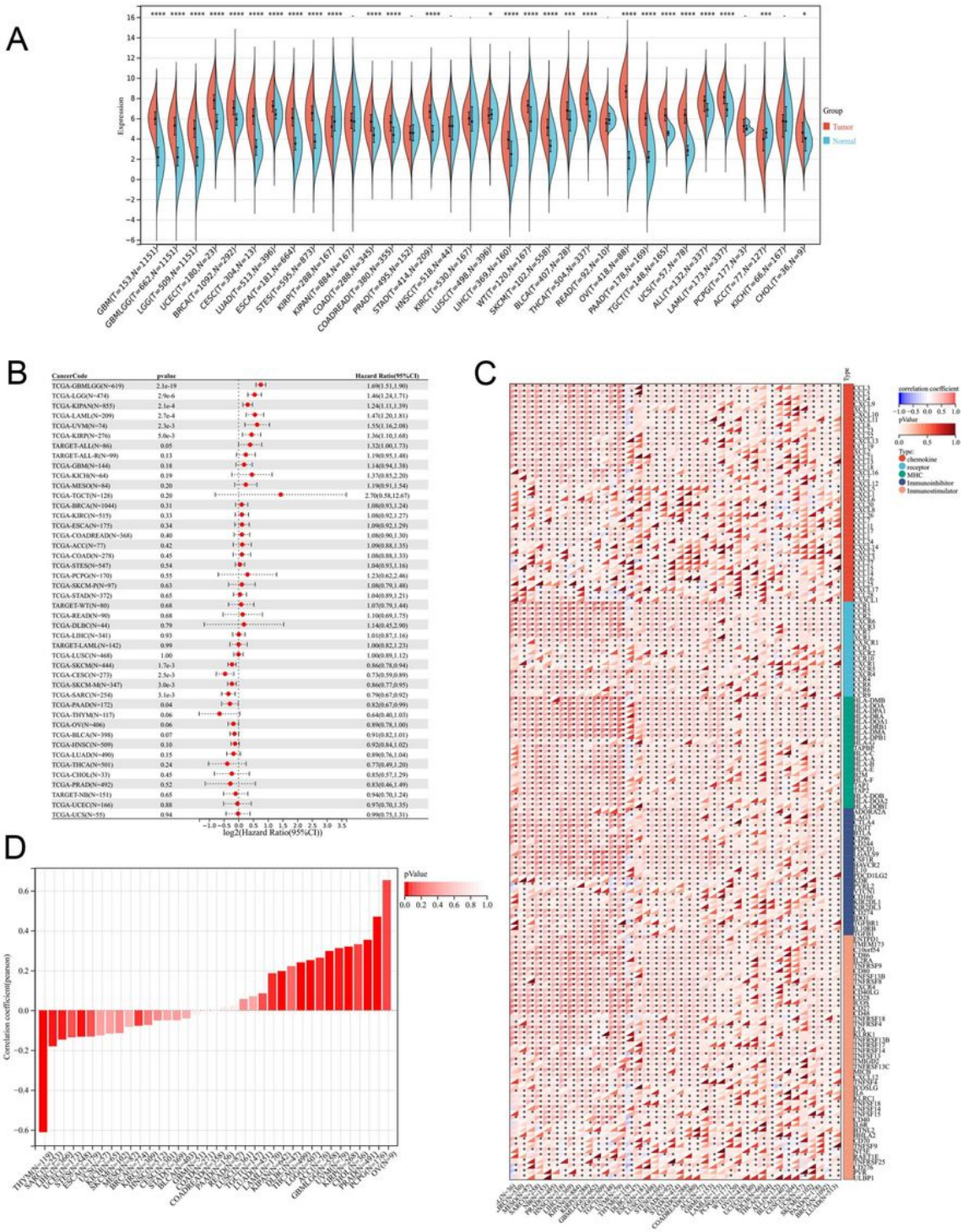

Figure 5

UCP2 pan-cancer immunoassay

(A) Differential expression of UCP2 in multiple tumors.

(B) Prognostic relevance of UCP2 in multiple tumors.

(C) Pearson correlation between UCP2 and marker genes of five types of immune pathways.

(D) Correlation between tumor stemness and UCP2 expression.

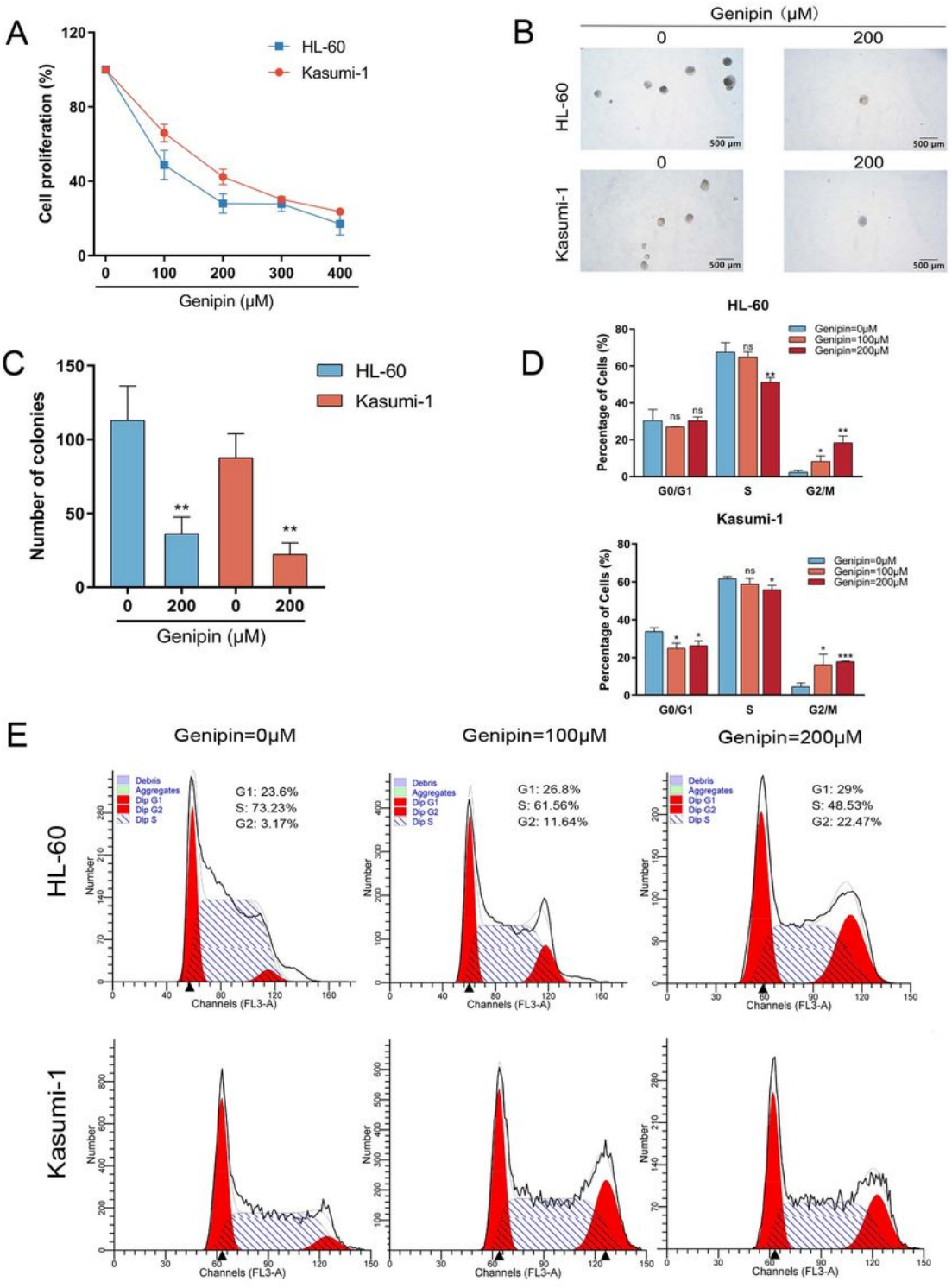

Figure 6

Genipin can effectively inhibit cellular activity in vitro and Genipin blocks the AML cell cycle in vitro

(A) The effect of Genipin on the viability of HL-60, and Kasumi-1 cells was measured by CCK-8 assay.

(B)(C) A colony formation assay was performed to examine the effect of Genipin on the proliferation of HL60, and Kasumi-1 cells.

(D)(E) Flow cytometry assay of the effect of Genipin on HL-60, Kasumi-1 cell cycle.

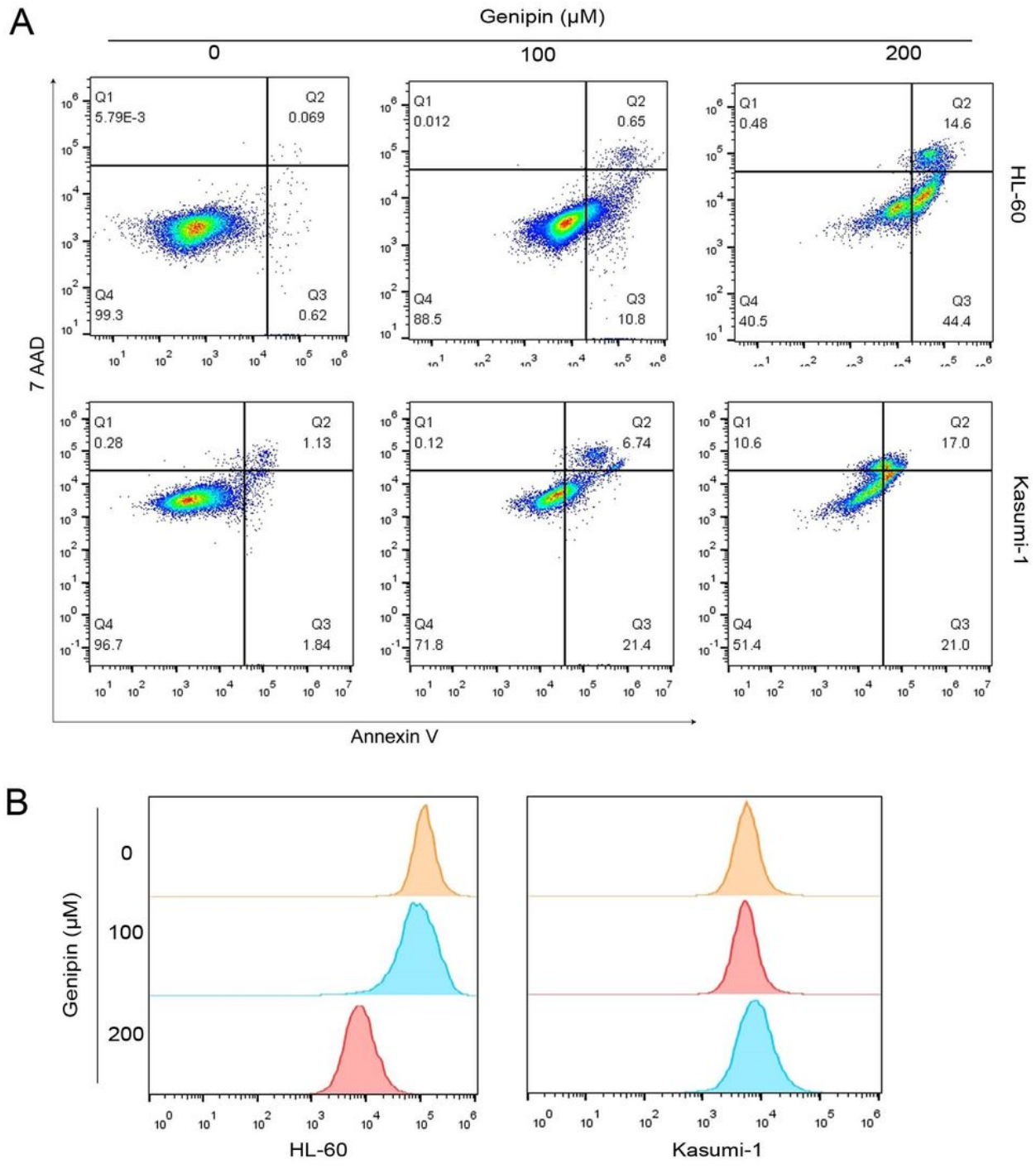

Figure 7

Genipin reduces the level of reactive oxygen species in AML cells and promotes apoptosis.

(A) Flow cytometric detection of the effect of Genipin on the apoptosis of HL-60, Kasumi-1 cells.

(B) Flow cytometry was performed to detect intracellular ROS levels in HL-60, Kasumi-1 cells after 6 hours of Genipin treatment.